Hindawi
Journal of Applied Mathematics
Volume 2024, Article ID 9943698, 17 pages
https://doi.org/10.1155/2024/9943698

Research Article

Enhancing Malaria Control Strategy: Optimal Control and Cost-Effectiveness Analysis on the Impact of Vector Bias on the Efficacy of Mosquito Repellent and Hospitalization

Iffatricia Haura Febiriana,[1,2] Abdullah Hasan Hassan,[1] and Dipo Aldila[1]

[1]*Department of Mathematics, Universitas Indonesia, Depok 16424, Indonesia*
[2]*Eijkman Research Center for Molecular Biology, National Research and Innovation Agency (BRIN), Cibinong, Indonesia*

Correspondence should be addressed to Dipo Aldila; aldiladipo@sci.ui.ac.id

Received 17 July 2023; Revised 31 January 2024; Accepted 15 February 2024; Published 15 March 2024

Academic Editor: Qiankun Song

Copyright © 2024 Iffatricia Haura Febiriana et al. This is an open access article distributed under the Creative Commons Attribution License, which permits unrestricted use, distribution, and reproduction in any medium, provided the original work is properly cited.

This paper focuses on the impact of mosquito biting bias on the success of malaria intervention strategies. The initial model is developed considering the existence of symptomatic and asymptomatic humans, as well as vector bias. The model is then analyzed to demonstrate how the malaria-endemic equilibrium always exists and is globally asymptotically stable if the basic reproduction number is larger than one. On the other hand, malaria will always go extinct in the population if the basic reproduction number is less than one. For intervention analysis, the model is extended by considering mosquito repellent and hospitalization as control strategies. The control reproduction number is shown analytically. Using the Pontryagin maximum principle, we characterize our optimal control problem. Several scenarios are conducted to observe the dynamics of control variables under different circumstances. We found that the intervention of mosquito repellent and hospitalization together is the most cost-effective strategy to reduce the spread of malaria. Furthermore, we have shown that the more biased the vector attracted to infected individuals, the higher the cost needed to implement the control strategy.

1. Introduction

The world harbors a wide array of infectious diseases, spanning those transmitted through direct human contact to those necessitating an intermediary animal or transmission through the environment. Diseases requiring an intermediary animal for transmission are also referred to as vector-borne diseases. Examples of such diseases encompass dengue, malaria, and chikungunya, among others. Malaria stands out as one of the most prevalent vector-borne diseases annually, particularly in Africa and Asia [1]. It prevails in tropical and subtropical regions globally, including Africa, Asia, and Latin America. Sub-Saharan Africa bears the heaviest burden in terms of malaria cases and fatalities [2].

Malaria is a life-threatening illness caused by the Plasmodium parasite, transmitted to humans through the bites of infected female Anopheles mosquitoes [3]. Typical malaria symptoms include high fever, chills, headache, sweating, fatigue, body aches, and nausea. If left untreated, it can progress to severe complications and potentially prove fatal [4]. Diagnosis of malaria can be achieved through laboratory tests that detect the presence of the parasite in the blood [5]. Early diagnosis and prompt treatment are crucial in preventing severe illness and death.

Effective malaria prevention strategies include the use of insecticide-treated bed nets, indoor residual spraying to eliminate mosquitoes, and antimalarial drugs for preventive treatment in high-risk areas [6–11]. The most effective treatment for uncomplicated malaria is artemisinin-based combination therapies (ACTs) [12]. However, the emergence of drug-resistant strains of the malaria parasite poses a significant challenge to malaria control efforts [13].

Another popular intervention for mosquito-borne diseases is the use of mosquito repellent, designed to deter mosquitoes from biting humans or animals. It operates by creating a barrier or emitting odors that repel mosquitoes,

thereby reducing the risk of mosquito-borne diseases and the discomfort of mosquito bites [14].

Global efforts to combat malaria have led to significant progress in reducing the disease burden. Increased funding, distribution of bed nets, improved access to diagnostic tests and treatment, and research on new prevention and treatment methods are crucial for further progress in malaria control and elimination.

Mathematical models have been employed by many researchers to comprehend how diseases may spread among populations, as demonstrated in references [15–18]. In the context of malaria transmission models, numerous approaches have been explored to assess how malaria spreads, considering factors such as vector bias [19, 20], repellent [21, 22], and treatment [23]. Some researchers also employ optimal control problems for malaria [24, 25] and cost-effectiveness methods to determine the best strategies for malaria prevention [26, 27]. Mojeeb and Li conducted a study on a mathematical malaria model, taking into account the effect of vector bias, and concluded that malaria could worsen if current control strategies are not improved [28]. Buonomo and Vargas-De-León introduced vector bias into their malaria transmission model and suggested that the greater attractiveness of infectious humans to mosquitoes plays a relevant role in malaria dynamics, especially when human immigration and death-induced mortality cannot be neglected [19]. Aldila and Seno [29] worked on a mathematical model of a general vector-borne disease with the presence of vector bias phenomena. The results obtained suggest that the control of disease becomes more challenging as the magnitude of vector bias increases. Overall, the discussed case ideas are intriguing, and the employed mathematical theories are deemed useful. However, it is noteworthy that the authors did not address optimal control models and cost-effectiveness, limiting the extent of conclusions that can be drawn for public health professionals. Unlike the work undertaken by Aldila and Angelina [30], their study involves the development of a malaria model incorporating vector bias along with optimal control simulations. However, it is essential to note that the proposed model has not yet discussed the asymptomatic cases in the malaria transmission process.

Based on the aforementioned information, it is evident that repellents and treatments play pivotal roles in mitigating the rapid transmission of malaria. Furthermore, there is a scarcity of mathematical models that consider the impact of vector bias on the efficacy of mosquito repellents and hospitalization in malaria control strategies. Consequently, we introduce a novel mathematical model to assess the influence of vector bias on the effectiveness of mosquito repellents and treatment in malaria eradication. We conduct optimal control problems utilizing repellents and treatments as controls and evaluate cost-effectiveness across various scenarios.

2. The Model Formulation

In this section, we formulate our malaria transmission model. We assume that the human population can be divided based on their health status as susceptible (S), asymptomatic infected (A), and symptomatic infected (I). Hence, the total population of humans is given by $N = S + A + I$. On the other hand, the mosquito population is divided only into two compartments, namely, susceptible (U) and infected (V) mosquitoes. Hence, the total mosquito population is given by $M = U + V$.

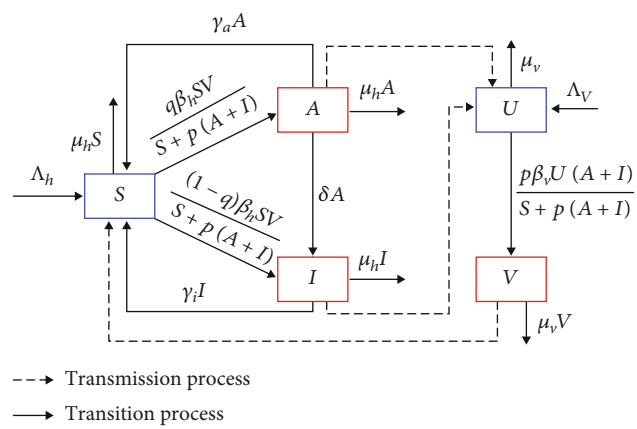

Figure 1: Transmission diagram of the malaria model in system (1).

The model is developed based on the transmission diagram in Figure 1 and the following assumptions. All newborn humans and mosquitoes are assumed to be always susceptible with a rate of Λ_h and Λ_v, respectively. Malaria infection only occurs due to the bite of infected mosquitoes on susceptible humans with a success rate of β_h, and the bite of susceptible mosquitoes on the infected humans A and I with a success rate of β_v. In 2005, Lacroix et al. [31] discovered that mosquitoes showed a greater attraction to individuals infected with malaria. Their research indicated that mosquitoes exhibited a heightened preference for humans carrying the transmissible gametocyte stage of malaria parasites, as opposed to those who were uninfected or had the nontransmissible asexual stages. This phenomenon is called vector bias. Hence, using a modification approach as the authors in [29, 30], with a vector-bias parameter $p > 1$, we model the infection process in humans and mosquitoes using a ratio-dependent term: $\beta_h SV/S + p(A+I)$ for humans and $\beta_v Up(A+I)/S + p(A+I)$ for mosquitoes. We assume that not all new infections of human which is denoted by $\beta_h SV/S + p(A+I)$ develop symptoms. Hence, we introduced q and $1-q$ as a proportion of new infected human who do not develop and develop symptoms, respectively. Therefore, we have $q\beta_h SV/S + p(A+I)$ goes to compartment A, while $(1-q)\beta_h SV/S + p(A+I)$ goes to compartment I.

Next, we have a recovery rate for asymptomatic and symptomatic infected individuals given by γ_a and γ_i, respectively. Furthermore, we assume that there is a progression of health status from asymptomatic to symptomatic individuals, called δ. Lastly, each compartment can decrease due to the natural death rate, namely, μ_h and μ_v for humans and mosquitoes, respectively. Hence, the mathematical model of malaria transmission, considering vector bias and

the asymptomatic phase, is given by the following system of five-dimensional ordinary differential equations.

$$\begin{aligned}
\frac{dS}{dt} &= \Lambda_h - \frac{\beta_h SV}{S+p(A+I)} - \mu_h S + \gamma_a A + \gamma_i I,\\
\frac{dA}{dt} &= \frac{q\beta_h SV}{S+p(A+I)} - \gamma_a A - \mu_h A - \delta A,\\
\frac{dI}{dt} &= \frac{(1-q)\beta_h SV}{S+p(A+I)} + \delta A - \gamma_i I - \mu_h I,\\
\frac{dU}{dt} &= \Lambda_v - \frac{p\beta_v U(A+I)}{S+p(A+I)} - \mu_v U,\\
\frac{dV}{dt} &= \frac{p\beta_v U(A+I)}{S+p(A+I)} - \mu_v V,
\end{aligned} \tag{1}$$

subject to the initial conditions $S(0) > 0$, $A(0) \geq 0$, $I(0) \geq 0$, $U(0) > 0$, and $V(0) \geq 0$. It is easy to show using an integrating factor method that each variable always has a nonnegative solution if the initial condition at $t = 0$ is also nonnegative.

2.1. Nondimensional Model. We assume the total of human and mosquito population is constant, then we have $S = N - A - I$ and $U = M - V$. Hence, system (1) now reads as

$$\begin{aligned}
\frac{dA}{dt} &= \frac{q\beta_h(N-A-I)V}{N-A-I+p(A+I)} - \gamma_a A - \mu_h A - \delta AS,\\
\frac{dI}{dt} &= \frac{(1-q)\beta_h(N-A-I)V}{N-A-I+p(A+I)} + \delta A - \gamma_i \mathrm{In} - \mu_h I,\\
\frac{dV}{dt} &= \frac{p\beta_v(M-V)(A+I)}{N-A-I+p(A+I)} - \mu_v V.
\end{aligned} \tag{2}$$

By substituting $x_1 = A/N$, $x_2 = I/N$ and $x_3 = V/M$ into system (2), we have

$$\begin{aligned}
\frac{dx_1}{dt} &= \frac{q\beta_h(1-x_1-x_2)x_3 M}{(1-x_1-x_2+p(x_1+x_2))N} - (\delta+\gamma_a+\mu_h)x_1,\\
\frac{dx_2}{dt} &= \frac{(1-q)\beta_h(1-x_1-x_2)x_3 M}{(1-x_1-x_2+p(x_1+x_2))N} + \delta x_1 - \gamma_i x_2 - \mu_h x_2,\\
\frac{dx_3}{dt} &= \frac{p\beta_v(1-x_3)(x_1+x_2)}{(1-x_1-x_2+p(x_1+x_2))} - \mu_v x_3.
\end{aligned} \tag{3}$$

Model in system (3) reduced our model from five to three dimensions. Hence, our model analysis will be focusing on system (3) instead of its original model in (1).

3. Model Analysis

Some mathematical analysis is given in this section, such as the existence of trivial and nontrivial equilibrium points, their stability, the basic reproduction number, and their global stability analysis.

3.1. Malaria-Free Equilibrium and the Basic Reproduction Number. The malaria-free equilibrium point (MFE) is a condition where malaria is no longer present in a population. Based on this definition, the malaria-free equilibrium point for system (3) is given by

$$\mathrm{MFE} = \left(x_1^0, x_2^0, x_3^0\right) = (0,0,0). \tag{4}$$

The basic reproduction number is determined from the spectral radius of the next-generation matrix of the respective model. We utilize the next-generation matrix approach [32] to determine the basic reproduction number of system (3). Readers may refer to [33–35] for more examples on the implementation of this method in the calculation of the reproduction number. The transition matrix (V) and transmission matrix (F) of system (3) are given by

$$V = \begin{bmatrix} -\delta-\gamma_a-\mu_h & 0 & 0\\ \delta & -\gamma_i-\mu_h & 0\\ 0 & 0 & -\mu_v \end{bmatrix},$$
$$F = \begin{bmatrix} 0 & 0 & \dfrac{q\beta_h M}{N}\\ 0 & 0 & \dfrac{(1-q)\beta_h M}{N}\\ (p)\beta_v & (p)\beta_v & 0 \end{bmatrix}. \tag{5}$$

Hence, the basic reproduction number is taken from the spectral radius of the next-generation matrix of system (3) which is given by

$$\mathscr{R}_0 = \sqrt{\frac{p\beta_v\beta_h M}{\mu_v N}\left(\frac{q}{\delta+\gamma_a+\mu_h} + \frac{\delta q}{(\delta+\gamma_a+\mu_h)(\gamma_i+\mu_h)} + \frac{1-q}{\gamma_i+\mu_h}\right)}. \tag{6}$$

To further interpret $\mathscr{R}_0$, equation (6) can be rewritten as follows:

$$\mathscr{R}_0^2 = \underbrace{\left(\frac{p\beta_v}{\mu_v}\right)}_{\text{Production of infected mosquito}} \underbrace{\beta_h\left(\frac{M}{N}\right)\left(\frac{q}{\delta+\gamma_a+\mu_h} + \frac{\delta q}{(\delta+\gamma_a+\mu_h)(\gamma_i+\mu_h)} + \frac{1-q}{\gamma_i+\mu_h}\right)}_{\text{Production of infected human}}. \tag{7}$$

It is clearly observed that $\mathscr{R}_0$ is a result of the multiplication of the number of newly infected mosquitoes and newly infected humans. Note that the production of infected human depends on the ration between mosquito and human. A larger ratio (larger population of mosquito) will increase the production of infected human.

Furthermore, it is not difficult to show that system (3) satisfies the five conditions in Theorem 3 [36]. Hence, using the result in [36], we have the following theorem.

Theorem 1. *The malaria-free equilibrium of system (3) (MFE) is always locally asymptotically stable if $\mathscr{R}_0 < 1$ and unstable if $\mathscr{R}_0 > 1$.*

3.2. Malaria-Endemic Equilibrium. The malaria endemic equilibrium (MEE) point of system (3) is given by

$$\mathrm{MEE} = (x_1^*, x_2^*, x_3^*), \tag{8}$$

where

$$\begin{aligned} x_1^* &= \frac{q x_2^* (\gamma_i + \mu_h)}{(1-q)\gamma_a + (1-q)\mu_h + \delta}, \\ x_3^* &= \frac{p\beta_v x_2^* ((1-q)\gamma_a + q\gamma_i + \delta + \mu_h)}{((1-q)\gamma_a + q\gamma_i + \delta + \mu_h)(\mu_v(p-1) + p\beta_v)x_2^* + \mu_v((1-q)\gamma_a + (1-q)\mu_h + \delta)}, \end{aligned} \tag{9}$$

while x_2^* is taken from the positive root of the following two-degree polynomial

$$F(x_2) = p_2 {x_2}^2 + p_1 x_2 + p_0 = 0, \tag{10}$$

with

$$\begin{aligned} p_2 &= qN(\gamma_i + \mu_h)(\delta + \gamma_a + \mu_h)((1-q)\gamma_a + q\gamma_2 + \delta + \mu_h)^2 \\ &\quad \cdot (p-1)(\mu_v(p-1) + p\beta_v), \\ p_1 &= q((1-q)\gamma_a + (1-q)\mu_h + \delta)((1-q)\gamma_a + q\gamma_i + \delta + \mu_h) \\ &\quad \cdot (Mp\beta_v((1-q)\gamma_1 + q\gamma_i + \delta + \mu_h)\beta_h + N(\gamma_i + \mu_h) \\ &\quad \cdot (\gamma_a + \delta + \mu_h)(p\beta_v + 2\,\mu_v(p-1))), \\ p_0 &= \left(1 - \mathscr{R}_0^2\right)(\gamma_i + \mu_h)(\delta + \gamma_a + \mu_h)(\mu_v N q)(\delta + (\gamma_a + \mu_h)(1-q)). \end{aligned} \tag{11}$$

From this, we can see if $\mathscr{R}_0 > 1$, then $p_0 < 0$. Hence, we have exactly one positive root of polynom 5 which indicates the existence of a unique endemic equilibrium for $\mathscr{R}_0 > 1$. On the other hand, if $\mathscr{R}_0 < 1$, then $p_0 > 0$. Hence, the multiplication of the root of system (10) will be positive, while the addition of the root will be negative since p_1 is always positive. Therefore, no endemic equilibrium if $\mathscr{R}_0 < 1$. These results are stated in the following theorem.

Theorem 2. *System (3) has a unique endemic equilibrium MEE if $\mathscr{R}_0 > 1$ and no endemic equilibrium otherwise.*

3.3. Bifurcation Analysis. In this section, we continue our analysis on the stability of the malaria endemic equilibrium from the previous section. From Theorem 2, we know that the endemic equilibrium is unique, and only appears when $\mathscr{R}_0 > 1$. To analyze the local stability of the malaria endemic equilibrium around $\mathscr{R}_0 = 1$, we will use the bifurcation theorem introduced by Castillo-Chavez and Song in [37]. First, we assumed β_h as the bifurcation parameter such that the critical value of β_h makes $\mathscr{R}_0 = 1$. With this, we have

$$\beta_h^* = \frac{(\delta + \gamma_a + \mu_h)(\gamma_i + \mu_h)\mu_v N}{p\beta_v M((1-q)\gamma_a + q\gamma_i + \delta + \mu_h)}. \tag{12}$$

Linearized system (3) around the malaria-free equilibrium and $\beta_h = \beta_h^*$ gives

$$\mathscr{A} = \begin{bmatrix} -\delta - \gamma_a - \mu_h & 0 & \dfrac{q(\gamma_i + \mu_h)(\delta + \gamma_a + \mu_h)\mu_v}{p\beta_v((1-q)\gamma_a + q\gamma_i + \delta + \mu_h)} \\ \delta & -\gamma_i - \mu_h & \dfrac{(1-q)(\gamma_i + \mu_h)(\delta + \gamma_a + \mu_h)\mu_v}{p\beta_v((1-q)\gamma_a + q\gamma_i + \delta + \mu_h)} \\ p\beta_v & p\beta_v & -\mu_v \end{bmatrix}. \tag{13}$$

It is easy to calculate the above matrix has a simple zero eigenvalue, while the other two are negative. Next, we calculated the right and left eigenvectors of the zero eigenvalues of $\mathscr{A}$ denoted by $w = (w_1, w_2, w_3)^T$ and $v = (v_1, v_2, v_3)$, respectively, which is given by

$$\begin{aligned} w_1 &= w_1, \\ w_2 &= \frac{((1-q)\gamma_a(1-q)\mu_h + \delta)w1}{(\gamma_i + \mu_h)q}, \\ w_3 &= \frac{w1\, p\beta_v((1-q)\gamma_a + q\gamma_i + \delta + \mu_h)}{q\mu_v(\gamma_i + \mu_h)}, \\ v_1 &= \frac{(\delta + \gamma_i + \mu_h)v2}{\delta + \gamma_a + \mu_h}, \\ v_2 &= v_2, \\ v_3 &= \frac{v2\,(\gamma_i + \mu_h)}{p\beta_v}. \end{aligned} \tag{14}$$

To use the Castillo-Chavez and Song theorem, we need to calculate the values of $\mathscr{A}$ and $\mathscr{B}$. The coefficient $\mathscr{A}$ is given as follows:

$$\begin{aligned} \mathscr{A} &= \sum_{k,i,j=1}^{3} v_k w_i w_j \frac{\partial^2 g_k}{\partial y_i \partial y_j}(\mathbf{0}, 0) = v_1 w_1 w_1 \frac{\partial^2 g_1}{\partial x_1 x_1}(\mathbf{0}, 0) \\ &\quad + v_1 w_1 w_2 \frac{\partial^2 g_1}{\partial x_1 x_2}(\mathbf{0}, 0) + \cdots + v_3 w_3 w_3 \frac{\partial^2 g_3}{\partial x_3 x_3}(\mathbf{0}, 0) \\ &= \frac{-a_1 - a_2}{a_3}, \end{aligned} \tag{15}$$

with

$$\begin{aligned} a_1 &= 2p^3\beta_v{}^2M((1-q)\gamma_a + q\gamma_i + \delta + \mu_h)^3\beta_h, \\ a_2 &= 2p\beta_v N^2(\gamma_i + \mu_h)(\delta + \gamma_a + \mu_h) \\ &\quad \cdot ((1-q)\gamma_a + q\gamma_2 + \delta + \mu_h)^2(p\beta_v + (p-1)\mu_v), \\ a_3 &= (\delta + \gamma_a + \mu_h)(\gamma_i + \mu_h)^2 q^2 \mu_v N p \beta_v. \end{aligned} \tag{16}$$

On the other hand, we have $\mathscr{B}$ as follows:

$$\begin{aligned} \mathscr{B} &= \sum_{k,i=1}^{3} v_k w_i \frac{\partial^2 g_k}{\partial y_i \partial \beta_h}(\mathbf{0}, 0) \\ &= v_1 w_3 \frac{\partial^2 g_1}{\partial x_3 \beta_h}(\mathbf{0}, 0) + v_2 w_3 \frac{\partial^2 g_2}{\partial x_3 \beta_h}(\mathbf{0}, 0) \\ &= \frac{\beta_v p((1-q)\gamma_a + q\gamma_2 + \delta + \mu_h)^2 M}{(\delta + \gamma_a + \mu_h)\mu_v(\gamma_i + \mu_h)Nq}. \end{aligned} \tag{17}$$

Since all parameters are positive, then we have $\mathscr{A} < 0$ and $\mathscr{B} > 0$. According to these results, the following theorem is obtained.

Theorem 3. *System (3) always exhibits a transcritical bifurcation at $\mathscr{R}_0 = 1$.*

With this theorem, we understand that the MEE is locally asymptotically stable when $\mathscr{R}_0 > 1$ but close to one. Furthermore, no backward bifurcation appears from system (3) at $\mathscr{R}_0 = 1$. Next, we show the global stability of the MEE.

3.4. Global Stability of the Endemic Equilibrium. We will apply the Dulac-Bendixson criterion [38] to show the global stability of the endemic equilibrium. Please see [39–43] for another example of this approach. Let $X = [x_1, x_2, x_3]$ be the open first octant. Now, we apply the Dulac-Bendixson criterion with $D = 1$ gives us

$$\begin{aligned} \frac{\partial f_1}{\partial x_1} + \frac{\partial f_2}{\partial x_2} + \frac{\partial f_3}{\partial x_3} = &-\frac{q\beta_h x_3 M}{(1 - x_1 - x_2 + p(x_1 + x_2))N} \\ &- \frac{q\beta_h(1 - x_1 - x_2)x_3 M(p-1)}{(1 - x_1 - x_2 + p(x_1 + x_2))^2 N} \\ &- \delta - \gamma_1 - 2\mu_h - \frac{(1-q)\beta_h x_3 M}{(1 - x_1 - x_2 + p(x_1 + x_2))N} \\ &- \frac{(1-q)\beta_h(1 - x_1 - x_2)x_3 M(p-1)}{(1 - x_1 - x_2 + p(x_1 + x_2))^2 N} \\ &- \gamma_i - \frac{p\beta_v(x_1 + x_2)}{1 - x_1 - x_2 + p(x_1 + x_2)} - \mu_v. \end{aligned} \tag{18}$$

Hence, we have $\partial f_1/\partial x_1 + \partial f_2/\partial x_2 + \partial f_3/\partial x_3 < 0$. It means we have the system strictly negative almost everywhere on Z. Thus, the system has no periodic orbits or graphics in the open first quadrant. Hence, by Poincare-Bendixson trichotomy Theorem 5.7 page 195 in [44], the endemic equilibrium MEE is global asymptotically stable.

3.5. Bifurcation Diagram and Autonomous Simulation. To illustrate the results of the bifurcation diagram, please refer to Figure 2. From Figure 2, it is evident that the endemic equilibrium x_2 exhibits a monotonically decreasing trend as β_h increases until it reaches the bifurcation point (BP) at $\mathscr{R}_0 = 1$ or $\beta_h = 0.012$. From the bifurcation diagram, we can see that there is a change in the stability of malaria-free equilibrium at BP, i.e., when $\mathscr{R}_0 = 1$, from stable to unstable. On the other hand, we have a new endemic equilibrium start to arise when the malaria-free equilibrium changes its stability. For five sample points of β_h when $\beta_h < 0.012$, the malaria-free equilibrium is stable, which is shown by the trajectories of the solution all tend to the malaria-free equilibrium (see Figure 2(b)). On the other hand, when we take five sample points when $\beta_h > 0.012$, then all the solutions tend to their own stable malaria-endemic equilibrium. See Figure 2(c) for the illustration. Larger β_h, then the size of x_2 at the equilibrium will become larger.

4. Optimal Control Problem

4.1. Optimal Control Model and Its Characterization. Here in this section, we introduce two different control variables to control the spread of malaria. Let $u_1(t)$ and $u_2(t)$ represent the use of mosquito repellent and hospitalization, respectively. Using ξ as the efficacy of mosquito repellent, then the reduction of effective contact rate β_h and β_v is given by $1 - u_1\xi$. Hence, the total of new infections in human and mosquito populations is given by $(1 - u_1(t)\xi)\beta_h SV/S + p(A + I)$ and $(1 - u_1(t)\xi)p\beta_v U(A + I)/S + p(A + I)$, respectively. Next, we assume that only proportion u_2 of symptomatic individuals following treatment in the hospital. Hence, their recovery rate (γ_t) will be larger than symptomatic individuals who are not treated in the hospital (γ_i). Hence, the total of recovered individual from the symptomatic class is given by $\gamma_t u_2(t)I + \gamma_i(1 - u_2(t))I$. Please note that $\gamma_t > \gamma_a > \gamma_i$. With this assumption, system (1) now reads as follows:

$$\begin{aligned} \frac{dS}{dt} &= \Lambda_h - \frac{(1 - u_1(t)\xi)\beta_h SV}{S + p(A + I)} - \mu_h S + \gamma_a A \\ &\quad + (\gamma_t u_2(t) + (1 - u_2(t))\gamma_i)I, \\ \frac{dA}{dt} &= q\frac{(1 - u_1(t)\xi)\beta_h SV}{S + p(A + I)} - \gamma_a A - \mu_h A - \delta A, \\ \frac{dI}{dt} &= (1-q)\frac{(1 - u_1(t)\xi)\beta_h SV}{S + p(A + I)}\Big) + \delta A - (\gamma_t u_2(t) + (1 - u_2(t))\gamma_i)I - \mu_h I, \\ \frac{dU}{dt} &= \Lambda_v - \frac{(1 - u_1(t)\xi)p\beta_v U(A + I)}{S + p(A + I)} - \mu_v U, \\ \frac{dV}{dt} &= \frac{(1 - u_1(t)\xi)p\beta_v U(A + I)}{S + p(A + I)} - \mu_v V. \end{aligned} \tag{19}$$

With the same approach as in the previous section, assuming $S = N - A - I$, $U = M - V$, $x_1 = A/N$, $x_2 = I/N$, and $x_3 = V/M$, we have

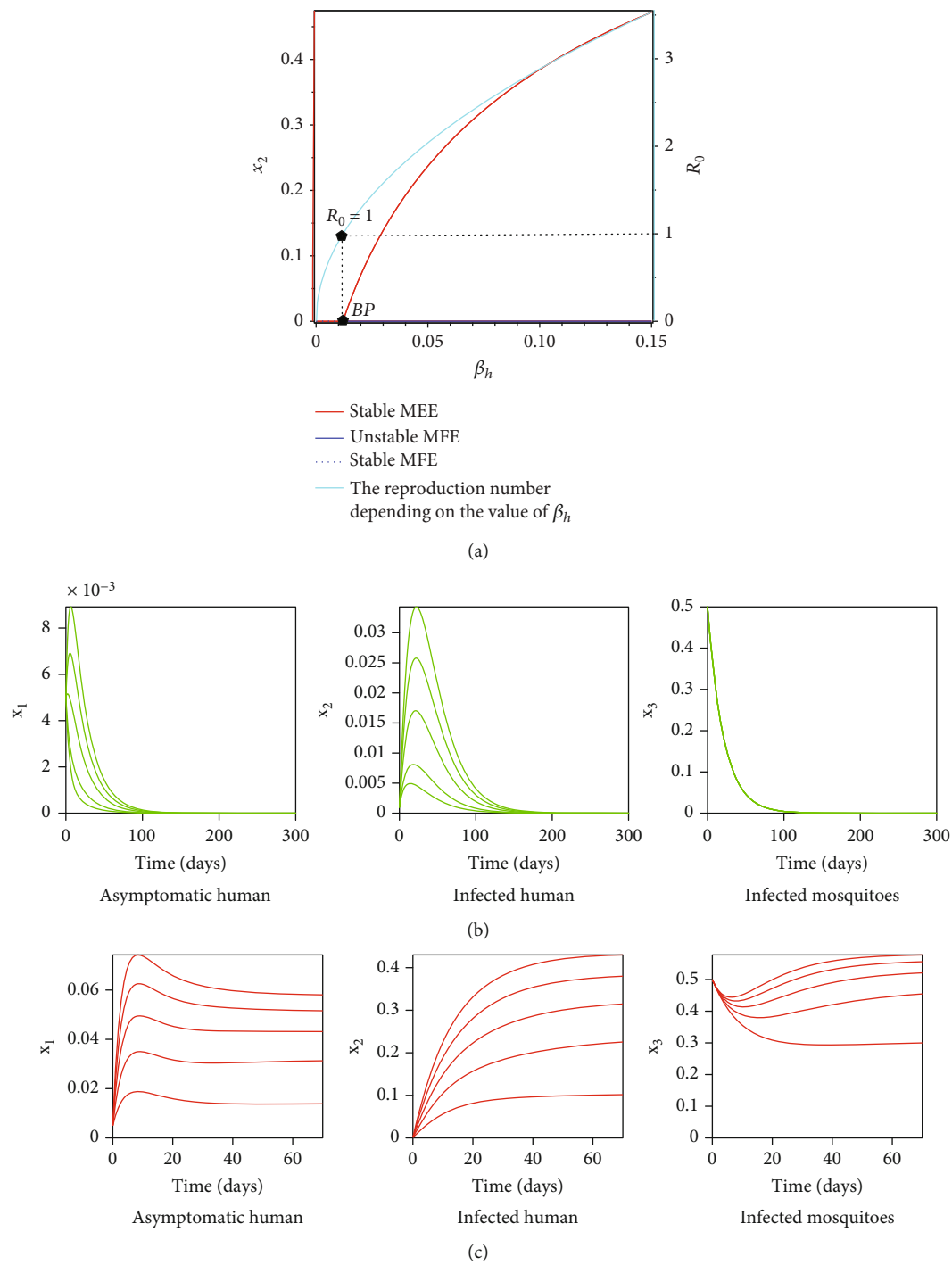

FIGURE 2: (a) Bifurcation diagram of x_2 respect to β_h. Solid red, blue, and cyan curves represent a stable endemic equilibrium, stable malaria-free equilibrium, and the reproduction number depending on the value of β_h. BP represent the bifurcation point at $\mathscr{R}_0 = 1$. (b) The dynamic of x_1, x_2, and x_3 tends to stable malaria-free equilibrium for all sample points such that $\mathscr{R}_0 < 1$. (c) The dynamic of x_1, x_2,and x_3 tends to stable malaria-endemic equilibrium for all sample points such that $\mathscr{R}_0 > 1$.

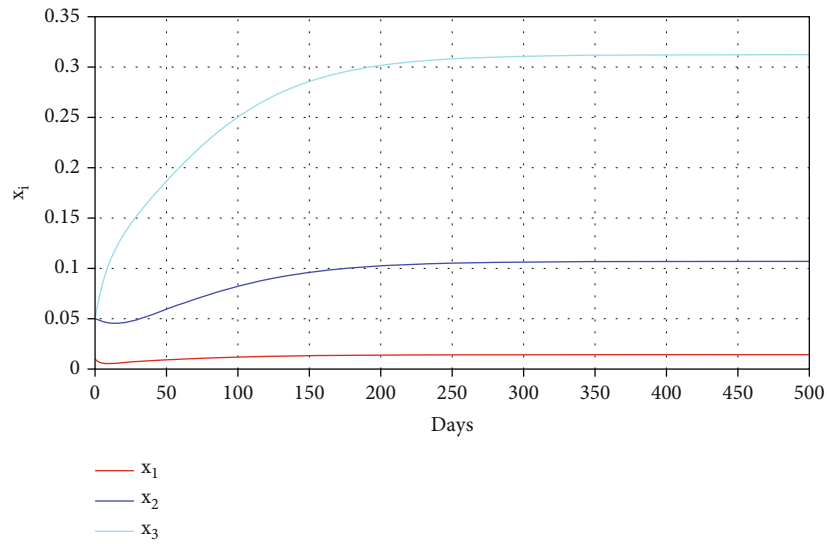

FIGURE 3: Dynamic of x_1, x_2, and x_3 tends to its malaria-endemic equilibrium for $\mathscr{R}_c > 1$.

$$\begin{aligned}
\frac{dx_1}{dt} &= \frac{q(1-u_1(t)\xi)\beta_h(1-x_1-x_2)x_3M}{(1-x_1-x_2+p(x_1+x_2))N} \\
&\quad - (\delta+\gamma_a+\mu_h)x_1, \\
\frac{dx_2}{dt} &= \frac{(1-q)(1-u_1(t)\xi)\beta_h(1-x_1-x_2)x_3M}{(1-x_1-x_2+p(x_1+x_2))N} \\
&\quad + \delta x_1 - (\gamma_t u_2(t) + (1-u_2(t))\gamma_i)x_2 - \mu_h x_2, \\
\frac{dx_3}{dt} &= \frac{p(1-u_1(t)\xi)\beta_v(1-x_3)(x_1+x_2)}{(1-x_1-x_2+p(x_1+x_2))} - \mu_v x_3.
\end{aligned} \tag{20}$$

Assuming $u_1(t) = u_1$ and $u_2(t) = u_2$, then the control reproduction number of system (20) is given by

$$\mathscr{R}_c = (1-u_1\xi)\sqrt{\frac{p\beta_v\beta_h M}{\mu_v N}\left(\frac{q}{\delta+\gamma_a+\mu_h} + \frac{\delta q}{(\delta+\gamma_a+\mu_h)(\bar{\gamma}_i+\mu_h)} + \frac{1-q}{\bar{\gamma}_i+\mu_h}\right)}, \tag{21}$$

where $\bar{\gamma}_i = (\gamma_t u_2 + (1-u_2)\gamma_i)$. From this expression, we can see that $\mathscr{R}_c(u_1 = 0, u_2 = 0) = \mathscr{R}_0$. Furthermore, we find that $\mathscr{R}_c \le \mathscr{R}_0$ for $u_1 \in [0,1]$ and $u_2 \in [0,1]$. Hence, we confidently can say that intervention with mosquito repellent and hospitalization have a good potential to reduce the spread of malaria.

Our aim is to minimize the proportion of infected individuals x_1 and x_2 with as minimum as possible cost of $u_1(t)$ and $u_2(t)$. This task is read as minimizing the following cost function.

$$J = \int_0^T \left(\omega_1 x_1 + \omega_2 x_2 + \frac{\omega_3}{2}u_1^2 + \frac{\omega_4}{2}u_2^2\right) dt, \tag{22}$$

where ω_1 and ω_2 are the weights of the objective functional for x_1 and x_2, respectively, while ω_3 and ω_4 for control variables u_1 and u_2, respectively. Next, by applying Pontryagin's maximum principle [45], we develop the Hamiltonian function as follows:

$$\begin{aligned}
H &= \omega_1 x_1 + \omega_2 x_2 + \frac{\omega_3}{2}u_1^2 + \frac{\omega_4}{2}u_2^2 \\
&\quad + \lambda_1\left(\frac{q(1-u_1(t)\xi)\beta_h(1-x_1-x_2)x_3M}{(1-x_1-x_2+p(x_1+x_2))N} - (\delta+\gamma_a+\mu_h)x_1\right) \\
&\quad + \lambda_2\left(\frac{(1-q)(1-u_1(t)\xi)\beta_h(1-x_1-x_2)x_3M}{(1-x_1-x_2+p(x_1+x_2))N}\right. \\
&\quad \left. + \delta x_1 - (\gamma_t u_2(t) + (1-u_2(t))\gamma_i)x_2 - \mu_h x_2\right) \\
&\quad + \lambda_3\left(\frac{p(1-u_1(t)\xi)\beta_v(1-x_3)(x_1+x_2)}{1-x_1-x_2+p(x_1+x_2)} - \mu_v x_3\right).
\end{aligned} \tag{23}$$

Thus, taking the partial derivatives of H with respect to each of the state variables yields the adjoint system given below:

$$\begin{aligned}
\frac{d\lambda_1}{dt} &= -\frac{\partial H}{\partial x_1} = -\omega_1 + (\lambda_1 - \lambda_2)\left(\frac{\beta_h(1-\xi u_1)x_3MpqN}{(1-x_1-x_2+p(x_1+x_2))^2N} + \delta\right) \\
&\quad + \lambda_1(\gamma_a+\mu_h) + \lambda_2\left(\frac{\beta_h(1-\xi u_1)x_3Mp}{(1-x_1-x_2+p(x_1+x_2))^2N}\right) \\
&\quad + \lambda_3\left(\frac{p\beta_v(1-\xi u_1)(1-x_3)}{(1-x_1-x_2+p(x_1+x_2))^2}\right),
\end{aligned} \tag{24}$$

$$\begin{aligned}
\frac{d\lambda_2}{dt} &= -\frac{\partial H}{\partial x_2} = -\omega_1 + (\lambda_1 - \lambda_2)\left(\frac{\beta_h(1-\xi u_1)x_3MpqN}{(1-x_1-x_2+p(x_1+x_2))^2N}\right) \\
&\quad + \lambda_2(u_2\gamma_t + (1-u_2)\gamma_i + \mu_h) + \lambda_3\left(\frac{p\beta_v(1-\xi u_1)(1-x_3)}{(1-x_1-x_2+p(x_1+x_2))^2}\right),
\end{aligned} \tag{25}$$

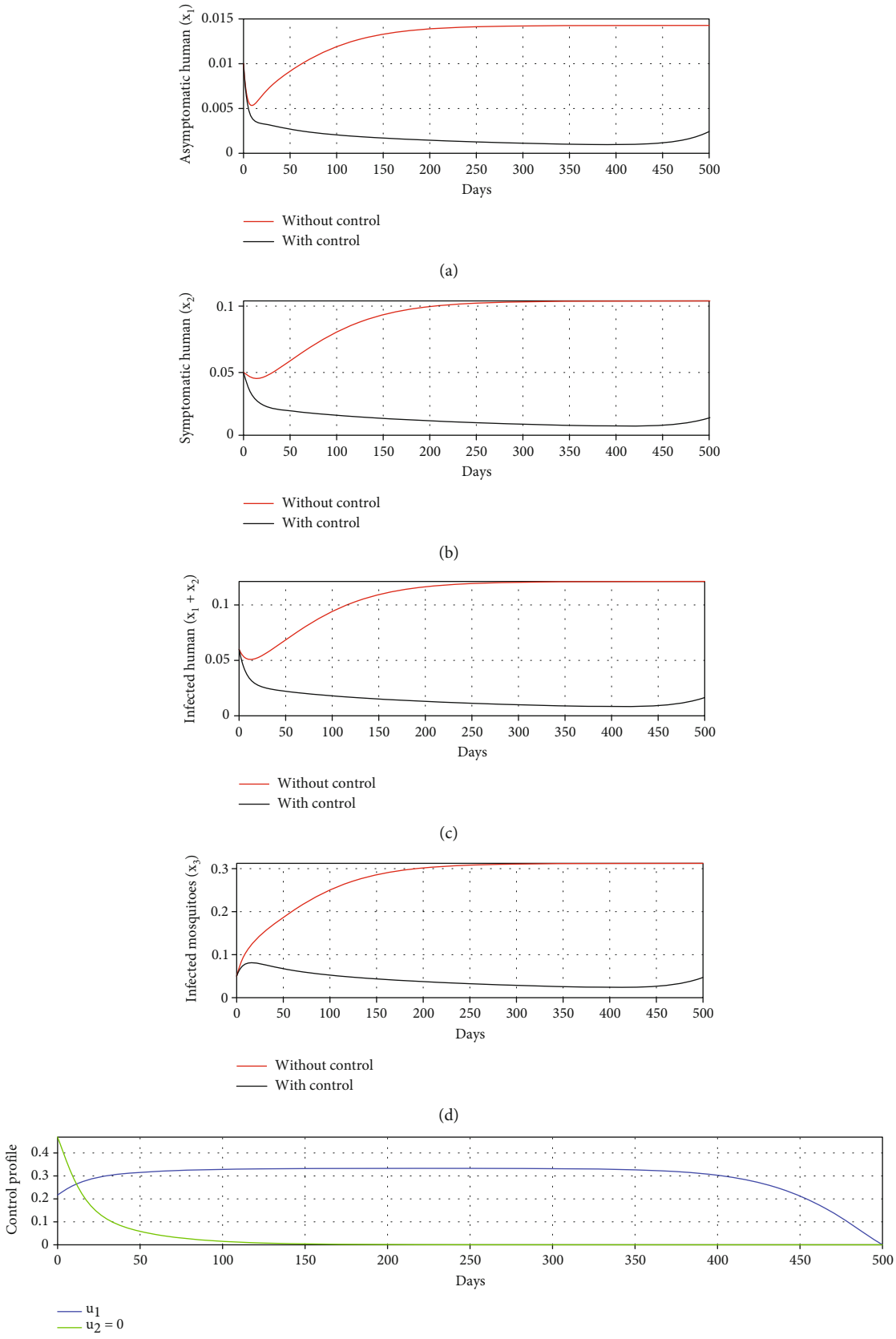

Figure 4: Scenario 1: use of repellent and hospitalization.

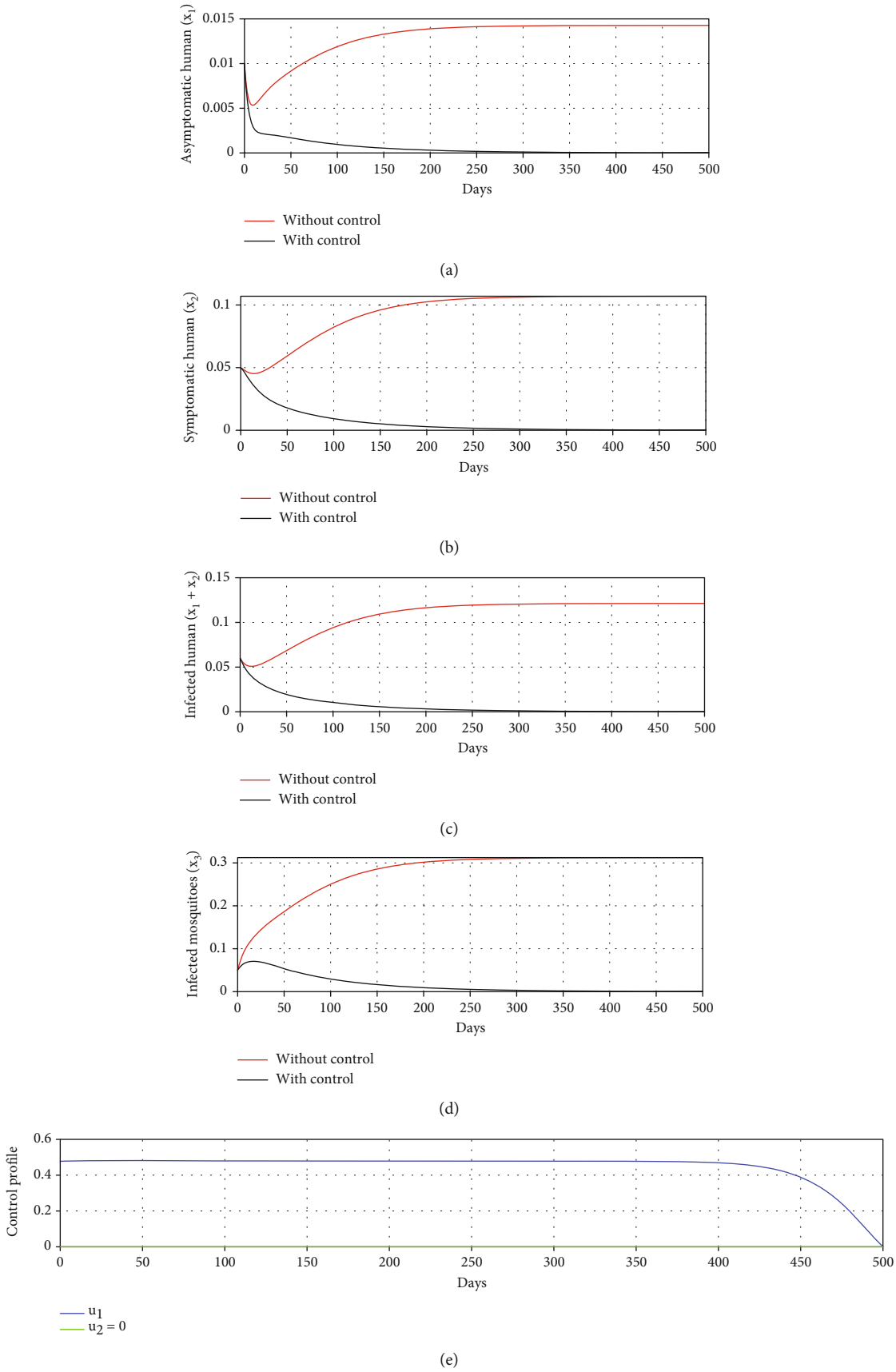

Figure 5: Scenario 2: use of repellent only.

$$\frac{d\lambda_3}{dt} = -\frac{\partial H}{\partial x_3} = (\lambda_2 - \lambda_1)\left(\frac{q\beta_h(-\xi u_1 + 1)(-x_1 - x_2 + 1)M}{(1 - x_1 - x_2 + p(x_1 + x_2))N}\right) - \lambda_2\left(\frac{\beta_h(-\xi u_1 + 1)(-x_1 - x_2 + 1)M}{(1 - x_1 - x_2 + p(x_1 + x_2))N}\right) + \lambda_3\left(\frac{p\beta_v(-\xi u_1 + 1)(x_1 + x_2)}{(1 - x_1 - x_2 + p(x_1 + x_2))} + \mu_v\right), \tag{26}$$

completed with the transversality condition $\lambda_i(t = T) = 0$ for $i = 1, 2, 3$. Further, the optimal controls (u_1^*, u_2^*) are given by

$$u_1^* = \min\left\{\max\left\{0, u_1^\dagger, 1\right\}\right., \tag{27a}$$

Table 1: The average cost-effectiveness ratio (ACER) of scenarios 1–3. Note: TAI = total averted infection; TCI = total costs for intervention.

Scenarios	Optimal control	TAI	TCI	ACER
1	u_1, u_2	0.0555	4.7×10^{-6}	8.4×10^{-5}
2	u_1	0.101	1.2×10^{-5}	1.2×10^{-4}
3	u_2	0.107	0.069	0.65

$$u_2^* = \min\left\{\max\left\{0, \frac{\lambda_2(\gamma_t - \gamma_i)x_2}{\omega_4}\right\}, 1\right\}, \tag{27b}$$

with

$$u_1^\dagger = \frac{(\lambda_1 - \lambda_2)((q\beta_h\xi(-x_1 - x_2 + 1)x_3M/(1 - x_1 - x_2 + p(x_1 + x_2))N)) + \lambda_2((\beta_h\xi(-x_1 - x_2 + 1)x_3M/(1 - x_1 - x_2 + p(x_1 + x_2))N)) + \lambda_3((\beta_v p\xi(1 - x_3)(x_1 + x_2)/(1 - x_1 - x_2 + p(x_1 + x_2))))}{\omega_3}\Bigg\}. \tag{28}$$

4.2. Optimal Control Simulation. This section shows the optimal scenario. We use the following parameter values to run the simulations, except it is stated differently:

$$\begin{aligned} M &= 10000, \\ N &= 10000, \\ p &= 2, \\ q &= 0.5, \\ \beta_h &= 0.025, \\ \beta_v &= 0.1, \\ \gamma_t &= \frac{1}{7}, \\ \gamma_a &= \frac{1}{14}, \\ \gamma_i &= \frac{1}{21}, \\ \delta &= \frac{1}{7}, \\ \mu_h &= \frac{1}{65 \times 265}, \\ \mu_v &= \frac{1}{21}. \end{aligned} \tag{29}$$

With these chosen parameter values, we have $\mathscr{R}_0(u_1 = 0, u_2 = 0) = 2.08$, indicating the stability of the endemic equilibrium point. Hence, without any intervention of controls, the population will tend to an endemic situation where the proportion of asymptomatic individuals reaches 1.4%, the proportion of symptomatic individuals reaches 10.6%, and the proportion of infected mosquitoes reaches 31.2%. The dynamics of system (20), which tend towards the endemic equilibrium point, are shown in Figure 3.

We solve the model in (20) with and without control numerically by applying the backward and forward sweep as described in [45]. Readers who are interested to see further examples on the implementation of this algorithm may refer to [33, 46–48]. In the beginning, we give an initial guess for $u_1(t)$ and $u_2(t)$ constant for all time t. With this initial guess, we solve system (20) forward in time. This solution is then used to solve the adjoint system in (24) backward in time. Hence, we can update the optimal value of $u_1(t)$ and $u_2(t)$ using the formula in (27a). We repeat these steps until we reach the convergence criteria or its maximum iteration K, i.e., $\|J^{\text{Iteration}-(k+1)} - J^{\text{Iteration}-(k)}\| < \varepsilon$, where ε is the tolerated error. We use $\omega_1 = 0.3$, $\omega_2 = 0.3$, $\omega_3 = 0.01$, and $\omega_4 = 0.1$ to run all of our optimal control simulation, except it is stated differently.

4.2.1. Different Combination of Interventions. In this section, we give three different scenarios of implementation for malaria eradication. The first scenario is when mosquito repellent and hospitalization are combined $(u_1 \neq 0, u_2 \neq 0)$, the second scenario is when we use hospitalization only ($u_1 = 0, u_2 \neq 0$), and the third scenario is when we use mosquito repellent only $(u_1 \neq 0, u_2 = 0)$. The results are given as follows.

(1) Scenario 1: use of repellent and hospitalization

As shown in Figure 4, the dynamic of asymptomatic humans, symptomatic humans, and infected mosquitoes decreases more rapidly when controls are used compared to the case without controls (see Figures 4(a)–4(d)). The control profiles in Figure 4(e) show that malaria can be controlled when we initially use u_2 maximally (47%) and then

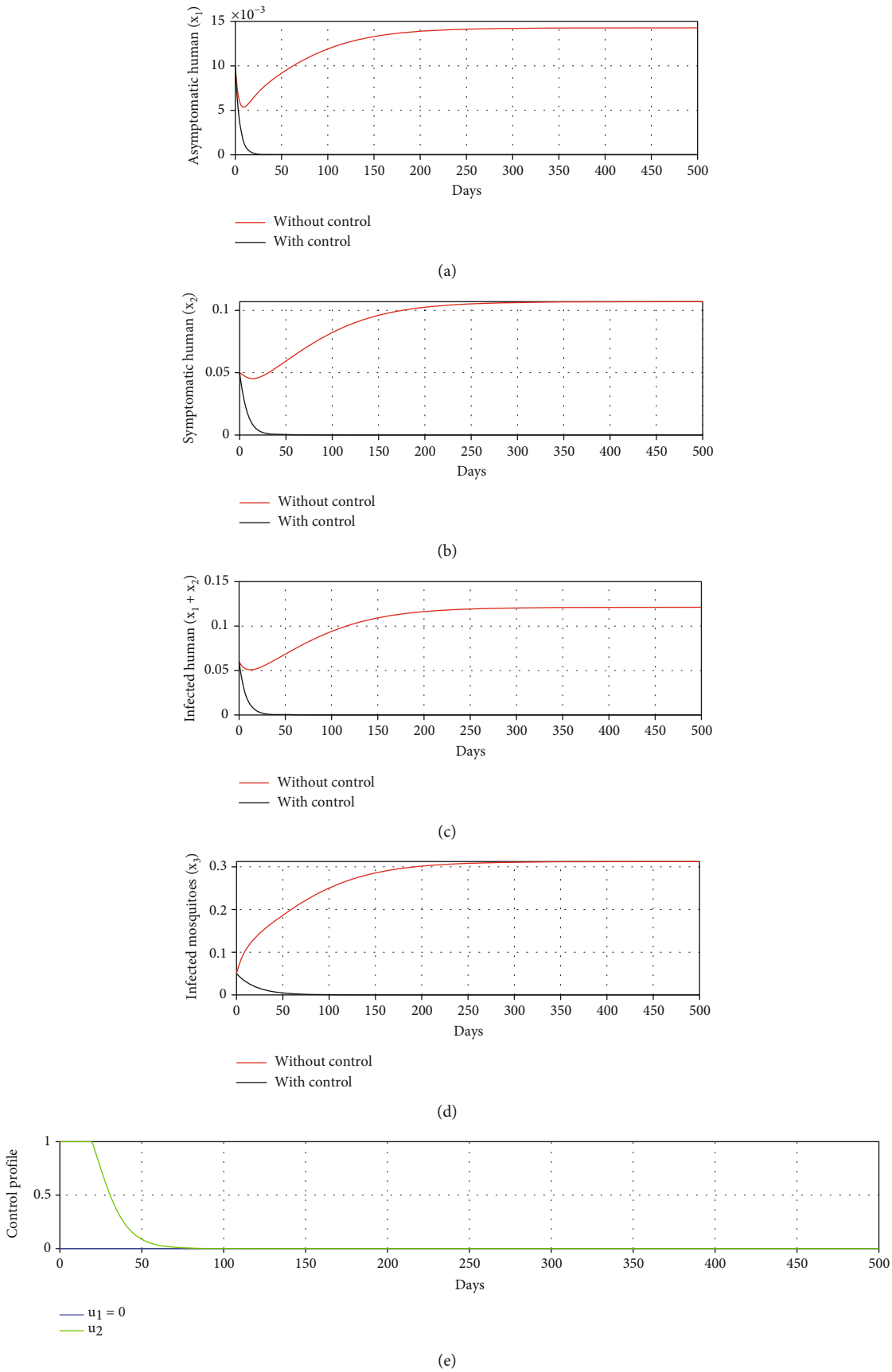

Figure 6: Scenario 3: use of hospitalization only.

rapidly decreased due to the reduction of infected individuals. On the other hand, we need to maintain u_1 at a nearly constant level throughout the simulation time (22%-33%), except at the beginning and at the end of the simulation time. This high intensity of mosquito repellent is implemented to prevent an increase in the proportion of infected individuals.

(2) Scenario 2: use of repellent only

Scenario 2 shows the strategy of using only repellent (u_1). As shown in Figures 5(a)–5(d), the proportions of asymptomatic humans, symptomatic humans, and infected mosquitoes significantly decrease compared to scenario 1. However, a high intensity of mosquito repellent, 48% for the majority of the simulation period, is required (please see Figure 5(e)). This implies that almost half of the population must consistently use mosquito repellent. This intervention comes with a higher cost of implementation. Please refer to Table 1 for detailed cost information.

(3) Scenario 3: use of hospitalization only

Scenario 3 shows the strategy of using only hospitalization (u_2 implemented to reduce malaria spread). Similarly, we can observe the success of hospitalization intervention in reducing the number of infected individuals. From Figures 6(a)–6(d), we can see a more significant reduction in the number of infected individuals and mosquitoes compared to other scenarios. However, it requires maximal intensity at the beginning of the simulation period, with 100% of symptomatic individuals being hospitalized. This high intensity of hospitalization leads to a significant increase in the implementation cost.

(1) Cost-Effectiveness Analysis. To determine the most cost-effective strategy from the three strategies, we conducted a cost-sensitivity analysis using the incremental cost-effectiveness ratio (ICER) and the most avoid the number of infected individuals at the cost of intervention the minimum (ACER) [49]. Table 1 shows the proportion of infections averted and the total cost for each scenario. The total proportion of averted infections was calculated using the following formula:

$$AI = \int_0^T \left[\sum_{i=1}^{3} \left(x_i\left(u_j \neq 0\right) - x_i\left(u_j = 0\right) \right) \right] dt, \tag{30}$$

Table 2: The average cost-effectiveness ratio (ICER) increasing order based on scenarios 1–3. Note: TAI = total averted infection; TCI = total costs for intervention.

Scenarios	Optimal control	TAI	TCI	ICER
1	u_1, u_2	0.0555	4.7×10^{-6}	8.5×10^{-5}
2	u_1	0.101	1.2×10^{-5}	1.6×10^{-4}
3	u_2	0.107	0.069	11.5

Table 3: The average cost-effectiveness ratio (ICER) increasing order based on scenarios 1 and 3. Note: TAI = total averted infection; TCI = total costs for intervention.

Scenarios	Optimal control	TAI	TCI	ICER
1	u_1, u_2	0.0555	4.7×10^{-6}	8.5×10^{-5}
2	u_1	0.101	1.2×10^{-5}	1.6×10^{-4}

for $j = 1, 2$. On the other hand, the total cost is given by equation $\int_0^T (\omega_3 u_1^2 + \omega_4 u_2^2) dt$. The results for each scenario are given in Table 1.

Next, we analyze the cost-effectiveness of two methods as follows:

(1) Average cost-effectiveness ratio (ACER)

The ACER represents the average cost that should be spent for each infected averted human. Hence, the formula for ACER is given by

$$\mathrm{ACER}_{\mathrm{scenario}-i} = \frac{\text{total cost for intervention with scenario} - i}{\text{total proportion of infection averted with scenario} - i}. \tag{31}$$

A smaller ACER indicates a better strategy of intervention. The results of the ACER values for each strategy are shown in Table 1. From Table 1, the best strategy based on the ACER index is the implementation of repellent and hospitalization (u_1 and u_2) as a double form intervention (scenario 1), followed with scenarios 2 and 3, respectively.

(2) The incremental cost-effectiveness ratio (ICER) formula

$$\mathrm{ICER}_{\mathrm{scenario}-(i,J)} = \frac{\text{difference of cost between scenario } i \text{ and scenario } j}{\text{difference of number of infection averted between scenario } i \text{ and scenario } j}. \tag{32}$$

Based on the numerical simulation, we rank all strategies in increasing order based on the total number of infections averted in Table 2.

Note that ICER for scenario 3 is larger than any other scenario. Hence, we can exclude ICER for scenario 3 from the next calculation. Next, we compare the ICER between

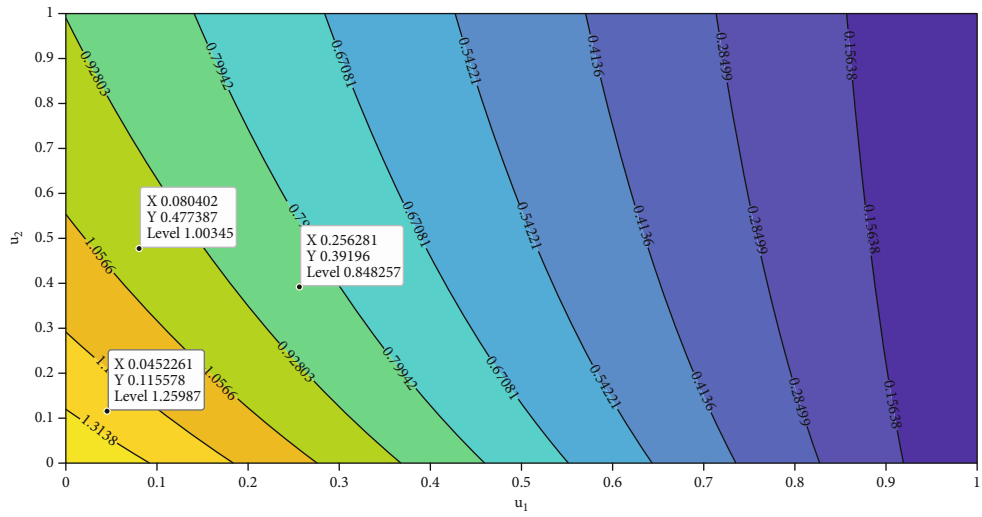

(a)

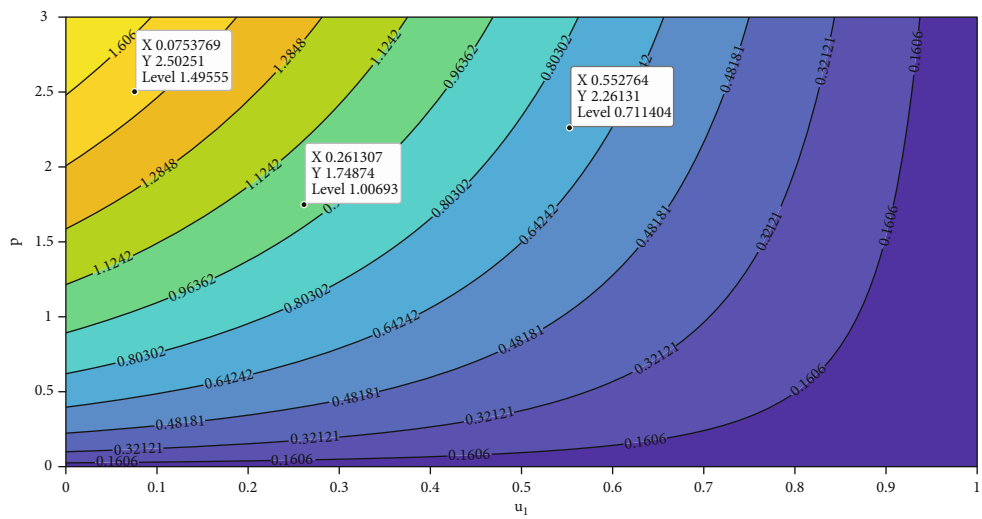

(b)

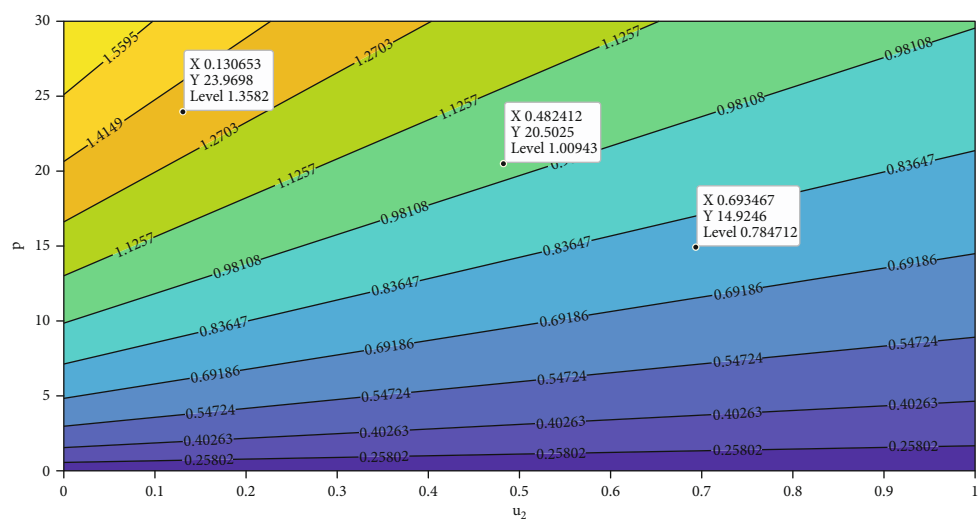

(c)

Figure 7: (a) Level set of $\mathscr{R}_c$ with respect to u_1 and u_2. (b, c) Impact of vector bias on the effectiveness of u_1 and u_2 to reduce $\mathscr{R}_c$.

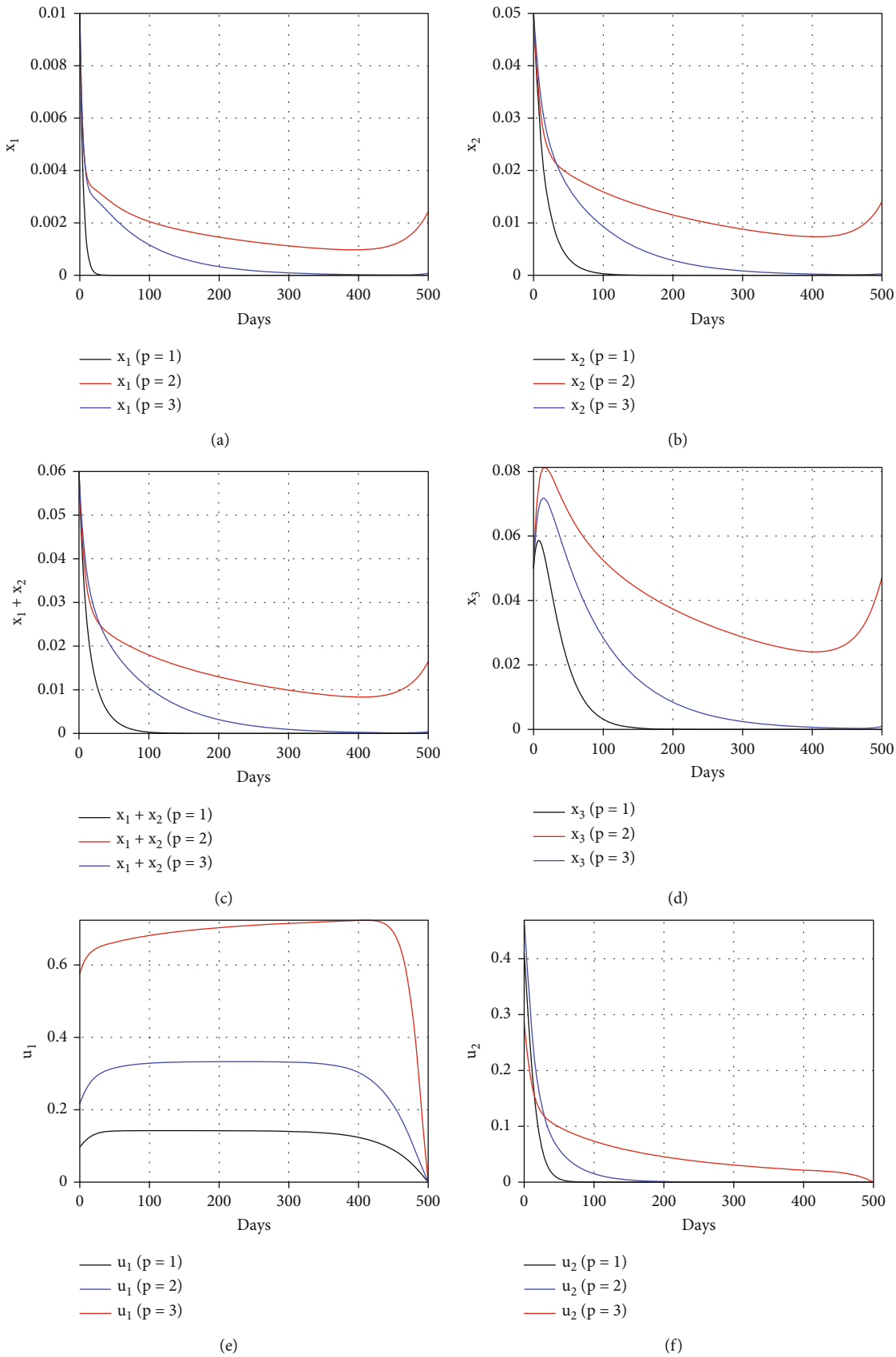

FIGURE 8: Optimal solution of system (20) for $p = 1, 2, 3$. (a–c) The proportion of infected individual x_1, x_2, and $x_1 + x_2$, respectively. (d) The dynamic with and without control of the mosquito population. (e, f) The dynamic of u_1 and u_2 for various value of p, respectively.

Table 4: Outcome of optimal control solution for different values of p.

	Case $p = 1$	Case $p = 2$	Case $p = 3$
$\mathscr{R}_0$	1.02	1.44	1.77
Total infected humans without control	0.00246	0.1075	0.2366
Total infected humans with control	0.00182	0.0141	0.0062
Total averted infected	6.4×10^{-4}	0.0934	0.2304
Percentage of reduction	26%	87%	97%
J	9.78×10^{-4}	0.0056	0.0069

scenarios 1 and 2. The result of calculating ICER using the same method as before is shown in Table 3.

Table 3 shows that ICER scenario 2 > ICER scenario 1, which means that scenario 2 (repellent (u_1)) is more costly compared to scenario 1 (combination of repellent u_1 and hospitalization (u_2) implemented). Hence, we can conclude that the use of repellent u_1 and hospitalization (u_1), as double intervention to reduce the spread of malaria, is the most cost-effective strategy compared to other possible scenarios.

4.2.2. Impact of Vector Bias on the Dynamic of Controls. In this section, we analyze the impact of vector bias on the dynamics of control variables. At first, we analyze the dependency of $\mathscr{R}_c$ to u_1 and u_2. By substituting all parameters in equation (27b), except u_1 and u_2 into $\mathscr{R}_c$, the level set of $\mathscr{R}_c$ respect to u_1 and u_2 is given in Figure 7. It can be seen clearly that increasing proportion of people who use mosquito repellent and infected people who undergo treatment in the hospital can reduce the control reproduction number $\mathscr{R}_c$ significantly (Figure 7(a)). Furthermore, from Figures 7(b) and 7(c), we can see that increasing of vector-bias parameter will increase the minimum effort of mosquito repellent and treatment such that $\mathscr{R}_c < 1$.

To study the impact of vector bias on the dynamics of malaria control, we computed the solutions of u_1 and u_2 for $p = 1, 2, 3$, as shown in Figure 8. Note that the basic reproduction number for each p is $\mathscr{R}_0(p = 1) = 1.02$, $\mathscr{R}_0(p = 2) = 1.44$, and $\mathscr{R}_0(p = 3) = 1.77$, indicating that without intervention (repellent or hospitalization), malaria will persist in the population.

The profiles of the controls appear similar for each value of p. However, a larger p requires a higher rate of repellent and hospitalization at all times t, resulting in a higher cost function value. For comparison, please refer to Table 4. It is clear that a higher value of vector bias necessitates a higher intensity of interventions, as indicated by a higher cost of J. This high intensity of intervention from the early period of the simulation leads to a greater reduction in the number of infected individuals. When $p = 3$, the percentage of infected individuals is reduced by 97% compared to the total infected without any control, whereas for $p = 2$ and $p = 1$, the reductions are 87% and 26%, respectively.

5. Conclusion

In this paper, we developed a nonstandard SAIS-UV model for malaria transmission. Unlike other malaria models [50–52], here, we consider a vector bias impact on the transmission process. As mentioned by [31], vector bias phenomena cannot be ignored in the malaria transmission process since it gives a higher preference to mosquitoes to bite infected humans. Unlike the proposed vector bias model by the author in [15, 29, 30, 53], here, we consider optimal control and asymptomatic cases in our analysis. With this model, infected humans are divided into two compartments, namely, asymptomatic and symptomatic individuals. With vector bias, mosquitoes are assumed to be more attracted to bite-infected humans. Mathematical analysis regarding its equilibrium points, global stability of the equilibrium points, and the basic reproduction number have been shown analytically. We found that malaria will always go extinct if the basic reproduction number is smaller than one. On the other hand, we always found a globally stable endemic equilibrium point if the basic reproduction number is larger than one. Furthermore, we also found that a larger vector bias of mosquitoes will increase the basic reproduction number.

For the malaria control strategy, we extend our model by involving two distinct interventions, namely, mosquito repellent (u_1) with an efficacy of $1 - \xi$ and hospitalization (u_2). In order to minimize the cost of intervention, we treat u_1 and u_2 as time-dependent variables. The Pontryagin maximum principle has been used to characterize the optimal control problem. Using cost-effectiveness analysis, we found that a combination of mosquito repellent and hospitalization is more cost-effective compared to other single interventions (hospitalization only or mosquito repellent only). Furthermore, we also found that the more biased vectors attracted to infected humans, the higher the cost needed to control the spread of malaria.

Although this model is simple in terms of the number of compartments involved, it can still provide us with insights into the importance of understanding the vector-bias phenomenon in malaria. Furthermore, we have not yet included other important factors such as people's awareness and fumigation to control the spread of malaria. Hence, we will consider these two interventions in future studies. Please refer to [54–56] for existing mathematical models on people awareness, media campaigns, and the use of Wolbachia in some vector-borne disease transmission models.

Data Availability

The data used to support this study is taken from the previously published papers.

Conflicts of Interest

The authors declare that there is no conflict of interest.

Acknowledgments

This research is funded by the Ministry of Education and Culture of Indonesia in collaboration with the Education Fund Management Institution (LPDP) of the Republic of Indonesia through the UKICIS Research Grant Scheme (ID number 4345/E4/AL.04/2022).

References

[1] R. E. Cibulskis, M. Aregawi, R. Williams, M. Otten, and C. Dye, "Worldwide incidence of malaria in 2009: estimates, time trends, and a critique of methods," *PLoS Medicine*, vol. 8, no. 12, article e1001142, 2011.

[2] World Health Organization (WHO), "Malaria," 2021, January 2022, https://www.who.int/news-room/fact-sheets/detail/malaria.

[3] C. Arama and M. Troye-Blomberg, "The path of malaria vaccine development: challenges and perspectives," *Journal of Internal Medicine*, vol. 275, no. 5, pp. 456–466, 2014.

[4] T. Harinasuta and D. Bunnang, "The clinical features of malaria," in *Malaria: Principles and Practice of Malariology*, W. H. Wernsdorfer and I. McGregor, Eds., pp. 709–734, Churchill Livingstone, London, 1988.

[5] B. Nkrumah, S. E. Acquah, L. Ibrahim et al., "Comparative evaluation of two rapid field tests for malaria diagnosis: Partec rapid malaria test and Binax Now malaria rapid diagnostic test," *BMC Infectious Diseases*, vol. 11, no. 1, pp. 1–8, 2011.

[6] S. I. Oke, M. M. Ojo, M. O. Adeniyi, and M. B. Matadi, "Mathematical modeling of malaria disease with control strategy," *Communications in Mathematical Biology and Neuroscience*, vol. 2020, 2020.

[7] R. J. Smith and S. D. Hove-Musekwa, "Determining effective spraying periods to control malaria via indoor residual spraying in sub-Saharan Africa," *Journal of Applied Mathematics and Decision Sciences*, vol. 2008, article 745463, pp. 1–19, 2008.

[8] F. O. Okumu and S. J. Moore, "Combining indoor residual spraying and insecticide-treated nets for malaria control in Africa: a review of possible outcomes and an outline of suggestions for the future," *Malaria Journal*, vol. 10, no. 1, pp. 1–3, 2011.

[9] N. Chitnis, A. Schapira, T. Smith, and R. Steketee, "Comparing the effectiveness of malaria vector-control interventions through a mathematical model," *The American Journal of Tropical Medicine and Hygiene*, vol. 83, no. 2, pp. 230–240, 2010.

[10] Q. Li and M. R. Hickman, *Pharmacokinetics and Pharmacodynamics of Antimalarial Drugs Used in Combination Therapy*, Bentham Science Publishers, 2015.

[11] W. Pongtavornpinyo, S. Yeung, I. M. Hastings, A. M. Dondorp, N. P. Day, and N. J. White, "Spread of anti-malarial drug resistance: mathematical model with implications for ACT drug policies," *Malaria Journal*, vol. 7, no. 1, pp. 1–12, 2008.

[12] M. Dhorda, C. Amaratunga, and A. M. Dondorp, "Artemisinin and multidrug-resistant plasmodium falciparum–a threat for malaria control and elimination," *Current Opinion in Infectious Diseases*, vol. 34, no. 5, pp. 432–439, 2021.

[13] S. Jana and J. Paliwal, "Novel molecular targets for antimalarial chemotherapy," *International Journal of Antimicrobial Agents*, vol. 30, no. 1, pp. 4–10, 2007.

[14] M. S. Fradin and J. F. Day, "Comparative efficacy of insect repellents against mosquito bites," *New England Journal of Medicine*, vol. 347, no. 1, pp. 13–18, 2002.

[15] D. Aldila, "Dynamical analysis on a malaria model with relapse preventive treatment and saturated fumigation," *Computational and Mathematical Methods in Medicine*, vol. 2022, Article ID 1135452, 19 pages, 2022.

[16] I. H. Febiriana, V. Adisaputri, P. Z. Kamalia, and D. Aldila, "Impact of screening, treatment, and misdiagnose on lymphatic filariasis transmission: a mathematical model," *Communications in Mathematical Biology and Neuroscience*, vol. 2023, 2023.

[17] D. Aldila, M. Z. Ndii, N. Anggriani, Windarto, H. Tasman, and B. D. Handari, "Impact of social awareness, case detection, and hospital capacity on dengue eradication in Jakarta: a mathematical model approach," *Alexandria Engineering Journal*, vol. 64, pp. 691–707, 2023.

[18] D. Aldila, J. P. Chavez, K. P. Wijaya, N. C. Ganegoda, G. M. Simorangkir, and H. Tasman, "A tuberculosis epidemic model as a proxy for the assessment of the novel $M72/AS01_E$ vaccine," *Communications in Nonlinear Science and Numerical Simulation*, vol. 120, article 107162, 2023.

[19] B. Buonomo and C. Vargas-De-León, "Stability and bifurcation analysis of a vector-bias model of malaria transmission," *Mathematical Biosciences*, vol. 242, no. 1, pp. 59–67, 2013.

[20] C. Vargas-De-León, "Global analysis of a delayed vector-bias model for malaria transmission with incubation period in mosquitoes," *Mathematical Biosciences and Engineering*, vol. 9, no. 1, pp. 165–174, 2012.

[21] A. E. Kiszewski and S. T. Darling, "Estimating a mosquito repellent's potential to reduce malaria in communities," *Journal of Vector Borne Diseases*, vol. 47, no. 4, pp. 217–221, 2010.

[22] Y. Thrower and L. I. Goodyer, "Application of insect repellents by travelers to malaria endemic areas," *Journal of Travel Medicine*, vol. 13, no. 4, pp. 198–202, 2006.

[23] M. Sinan, H. Ahmad, Z. Ahmad et al., "Fractional mathematical modeling of malaria disease with treatment & insecticides," *Results in Physics*, vol. 34, article 105220, 2022.

[24] F. Al Basir and T. Abraha, "Mathematical modelling and optimal control of malaria using awareness-based interventions," *Mathematics*, vol. 11, no. 7, p. 1687, 2023.

[25] J. P. Romero-Leiton, J. E. Castellanos, and E. Ibargün-Mondragón, "An optimal control problem and cost-effectiveness analysis of malaria disease with vertical transmission applied to San Andrés de Tumaco (Colombia)," *Computational and Applied Mathematics*, vol. 38, no. 3, pp. 1–24, 2019.

[26] M. A. Penny, R. Verity, C. A. Bever et al., "Public health impact and cost-effectiveness of the RTS, S/AS01 malaria vaccine: a systematic comparison of predictions from four mathematical models," *The Lancet*, vol. 387, no. 10016, pp. 367–375, 2016.

[27] P. Winskill, P. G. Walker, J. T. Griffin, and A. C. Ghani, "Modelling the cost-effectiveness of introducing the RTS, S malaria vaccine relative to scaling up other malaria interventions in sub-Saharan Africa," *BMJ Global Health*, vol. 2, no. 1, article e000090, 2017.

[28] A. L. Mojeeb and J. Li, "Analysis of a vector-bias malaria transmission model with application to Mexico, Sudan and

Democratic Republic of the Congo," *Journal of Theoretical Biology*, vol. 464, pp. 72–84, 2019.

[29] D. Aldila and H. Seno, "A population dynamics model of mosquito-borne disease transmission, focusing on mosquitoes' biased distribution and mosquito repellent use," *Bulletin of Mathematical Biology*, vol. 81, no. 12, pp. 4977–5008, 2019.

[30] D. Aldila and M. Angelina, "Optimal control problem and backward bifurcation on malaria transmission with vector-bias," *Heliyon*, vol. 7, no. 4, article e06824, 2021.

[31] R. Lacroix, W. R. Mukabana, L. C. Gouagna, and J. C. Koella, "Malaria infection increases attractiveness of humans to mosquitoes," *PLoS Biology*, vol. 3, no. 9, article e298, 2005.

[32] O. Diekmann, J. A. Heesterbeek, and M. G. Roberts, "The construction of next-generation matrices for compartmental epidemic models," *Journal of the Royal Society Interface*, vol. 7, no. 47, pp. 873–885, 2010.

[33] D. Aldila, B. D. Handari, A. Widyah, and G. Hartanti, "Strategies of optimal control for HIV spreads prevention with health campaign," *Communications in Mathematical Biology and Neuroscience*, vol. 2020, p. 7, 2020.

[34] D. Aldila, N. Nuraini, and E. Soewono, "Optimal control problem in preventing of swine flu disease transmission," *Applied Mathematical Sciences*, vol. 8, no. 71, pp. 3501–3512, 2014.

[35] D. Aldila, N. Rarasati, N. Nuraini, and E. Soewono, "Optimal control problem of treatment for obesity in a closed population," *International Journal of Mathematics and Mathematical Sciences*, vol. 2014, Article ID 273037, 7 pages, 2014.

[36] P. Van den Driessche and J. Watmough, "A simple SIS epidemic model with a backward bifurcation," *Journal of Mathematical Biology*, vol. 40, no. 6, pp. 525–540, 2000.

[37] C. Castillo-Chavez, B. Song, Mathematics, Computational and Modeling Sciences Center, Arizona State University, PO Box 871904, Tempe, AZ 85287, and Department of Mathematical Sciences, Montclair State University, Upper Montclair, NJ 07043, "Dynamical models of tuberculosis and their applications," *Mathematical Biosciences and Engineering*, vol. 1, no. 2, pp. 361–404, 2004.

[38] Y. Li and J. S. Muldowney, "On Bendixson' s criterion," *Journal of Differential Equations*, vol. 106, no. 1, pp. 27–39, 1993.

[39] A. Ayalew, Y. Molla, T. Tilahun, and T. Tesfa, "Mathematical model and analysis on the impacts of vaccination and treatment in the control of the COVID-19 pandemic with optimal control," *Journal of Applied Mathematics*, vol. 2023, Article ID 8570311, 15 pages, 2023.

[40] M. T. Hoang, "Dynamical analysis of a generalized hepatitis B epidemic model and its dynamically consistent discrete model," *Mathematics and Computers in Simulation*, vol. 205, pp. 291–314, 2023.

[41] O. Adebimpe, B. O. Moses, and O. J. Okoro, "Global stability analysis of a SEIR epidemic model with saturation incidence rate," *International Journal of Mathematical Sciences*, vol. 34, no. 1, 2014.

[42] Q. A. Dang and M. T. Hoang, "Complete global stability of a metapopulation model and its dynamically consistent discrete models," *Qualitative Theory of Dynamical Systems*, vol. 18, no. 2, pp. 461–475, 2019.

[43] J. Zhang and G. Feng, "Global stability for a tuberculosis model with isolation and incomplete treatment," *Computational and Applied Mathematics*, vol. 34, no. 3, pp. 1237–1249, 2015.

[44] L. J. S. Allen, *An Introduction to Mathematical Biology*, Pearson/Prentice Hall, 1st edition, 2007.

[45] S. Lenhart and J. T. Workman, *Optimal Control Applied to Biological Models*, Chapman & Hall/CRC Mathematical and Computational Biology Series, New York, 2007.

[46] B. D. Handari, R. A. Ramadhani, C. W. Chukwu, S. H. A. Khoshnaw, and D. Aldila, "An optimal control model to understand the potential impact of the new vaccine and transmission-blocking drugs for malaria: a case study in Papua and West Papua, Indonesia," *Vaccine*, vol. 10, no. 8, p. 1174, 2022.

[47] H. Tasman, D. Aldila, P. A. Dumbela et al., "Assessing the impact of relapse, reinfection and recrudescence on malaria eradication policy: a bifurcation and optimal control analysis," *Tropical Medicine and Infectious Disease*, vol. 7, no. 10, p. 263, 2022.

[48] D. Aldila, "Optimal control for dengue eradication program under the media awareness effect," *International Journal of Nonlinear Sciences and Numerical Simulation*, vol. 24, no. 1, pp. 95–122, 2023.

[49] F. B. Agusto and M. C. A. Leite, "Optimal control and cost-effective analysis of the 2017 meningitis outbreak in Nigeria," *Infectious Disease Modelling*, vol. 4, pp. 161–187, 2019.

[50] B. D. Handari, F. Vitra, R. Ahya, S. T. Nadya, and D. Aldila, "Optimal control in a malaria model: intervention of fumigation and bed nets," *Advances in Difference Equations*, vol. 2019, no. 1, 2019.

[51] B. D. Handari, A. Amalia, S. A. Rahmayani, and D. Aldila, "Numerical simulation of malaria transmission model considering secondary infection," *Communications in Mathematical Biology and Neuroscience*, vol. 2020, p. 36, 2020.

[52] B. D. Handari, D. Aldila, E. Tamalia, S. H. A. Khoshnaw, and M. Shahzad, "Assessing the impact of medical treatment and fumigation on the superinfection of malaria: a study of sensitivity analysis," *Communication in Biomathematical Sciences*, vol. 6, no. 1, pp. 51–73, 2023.

[53] F. Chamchod and N. F. Britton, "Analysis of a vector-bias model on malaria transmission," *Bulletin of Mathematical Biology*, vol. 73, no. 3, pp. 639–657, 2011.

[54] M. Z. Ndii and Y. A. Adi, "Understanding the effects of individual awareness and vector controls on malaria transmission dynamics using multiple optimal control," *Chaos, Solitons & Fractals*, vol. 153, article 111476, 2021.

[55] M. Z. Ndii, "The effects of vaccination, vector controls and media on dengue transmission dynamics with a seasonally varying mosquito population," *Results in Physics*, vol. 34, article 105298, 2022.

[56] M. Z. Ndii, L. K. Beay, N. Anggriani, K. N. Nukul, and B. S. Djahi, "Estimating the time reproduction number in Kupang City Indonesia, 2016–2020, and assessing the effects of vaccination and different Wolbachia strains on dengue transmission dynamics," *Mathematics*, vol. 10, no. 12, p. 2075, 2022.